Modeling and Path Tracking for Articulated Steering Vehicles

Fengqian Dou[1] , Wei Liu[2] , Yanjun Huang[3], Li Liu[1], Yu Meng[1*]

1. School of Mechanical Engineering
University of Science and Technology
Beijing, China

2. School of Mechanical Engineering
Beijing Institute of Technology
Beijing, China

3. Department of Mechanical and
Mechatronics Engineering
University of Waterloo
Waterloo, Canada

***Abstract*—This paper presents an integrated articulated steering vehicle's (ASV) dynamics model, which provides a simulation platform for research on path tracking control of ASV. The active speed limiting control is designed according to the sideslip constraints to improve the lateral stability of the vehicle during path tracking. The weighted PID controller is applied to control the steering torque based on the path tracking error. The model and the effect of the path-tracking controller are validated through the Matlab/Simulink simulation.**

Keywords—articulated steering vehicle; dynamic model, path tracking

I. INTRODUCTION

Articulated steer vehicles (ASVs) are widely applied in the forestry, construction, agriculture and mining industry. With the application of new technologies, the articulated steering vehicles have become an active research in recent decades, which mainly focus on the improving of efficiency and safety of the vehicles. [1, 2]. Recently, autonomous vehicles have attracted lots of attention from the automotive industry due to their potential applications in path tracking. However, fully autonomous driving for the ASVs is still a complex task. Therefore, the achievement on the fully autonomy should be the development trend of ASVs in the following decades, especially in the field of autonomous driving, since it has the it has the potential to improve safety by removing people from the vehicles, while simultaneously increasing productivity [3].

The first step of the path control problems is to get the accurate dynamics model of ASV. For the ASVs the steering process is achieved by two hydraulic cylinders. Owing ti their off road applications, these vehicles usually have powerful engine, and their powertrains are designed to produce extremely high driving torques at the wheels. In past decades, a few paper about the articulated steer vehicle model is presented. In [4], A linear, state-space, mathematical model of the vehicle is derived purely from geometric consideration of the vehicle and its desired path. Autonomous regulation of the vehicle is shown to be theoretically feasible using state variable feedback of displacement, heading angle, and curvature error. However, the dynamics of ASV is not considered in the paper. In [5], dynamics and kinematic modelling techniques including slip and no-slip models of articulated steer vehicle are discussed. In [6], a simple dynamical model is derived for the motion of a load,

haul, and dump truck (LHD) on a horizontal plane. In [7], the MPC controller is used to control the lateral motion of the vehicle, through the rate of the articulation angle, just based on the kinematics model. The dynamics model of ASV is nonlinear, and complex. Therefore, most research on path tracking for ASV, are mainly based on the kinematic model, which is not accurate. In [8], a linearized ASV dynamic model is used for the snaking-mode control. The main goal of path tracking control is to guide the autonomous vehicles along the reference or planned path. The widely used methods for path tracking of autonomous vehicles are mainly based on error dynamics models. In [9], the sliding-mode control was presented. In [10, 11], the fuzzy logic control and robust control were applied into the path tracking problems. In this paper, a 4 degree of freedom ASV dynamics model is built in Matlab/Simulink. The active speed limiting control and weighted PID control are applied to the path tracking for ASV.

The remainder of this paper is organized as follows. In section Ⅱ, the dynamics model of ASV is presented. The proposed path tracking control is presented in section Ⅲ. Section Ⅳ conducts simulation to verify the dynamics model and the proposed control strategy. Finally, the conclusions are provided in section Ⅴ.

II. SIMULATION PLATFORM FOR ARTICULATED STEERING VEHICLE

For the ASVs, they include two separate segments that are connected by the articulation joint, as shown in Fig 1. In this paper, a simulation platform was set up for ASV.

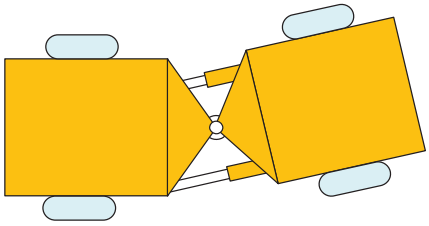

Fig. 1. Structure of articulated steering vehicle.

This work is supported by National High Technology Research and Development Program (863 Program) (No. 2011AA060408); National Key Technology Research and Development Program, (No. 2013BAB02B07); China Scholarship Council (No. 201606460035).

The structure of the simulation platform is shown as Fig.2. The whole model include the steering system model, wheel model, tire model, terrain model, auxiliary calculation model and vehicle body model.

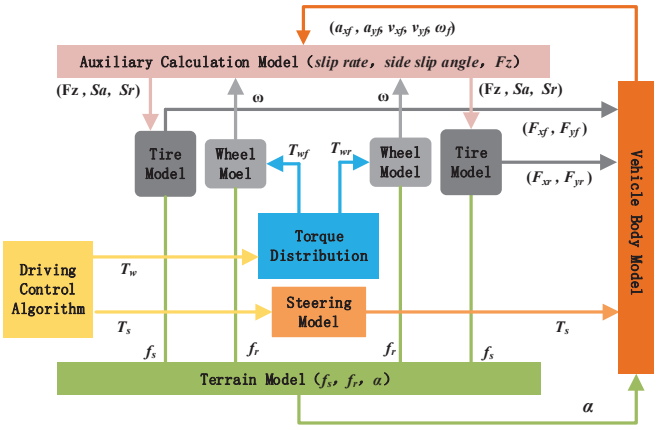

Fig. 2. Simulation platform of ASV.

A. Steering system modeling

The steering process of the ASV is achieved by controlling the flow of hydraulic fluid from the pump to the steering rams, as shown in Fig. 3.

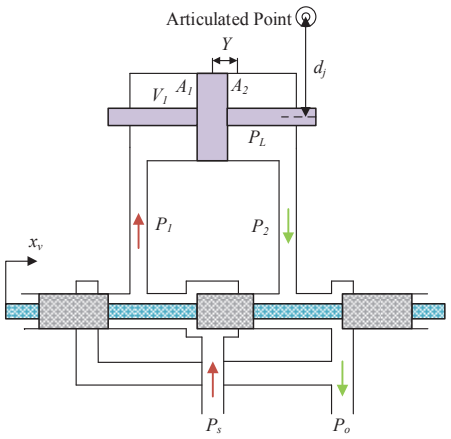

Fig. 3 The hydraulic steering system of ASV.

The valve displacement is x_v , the flow rates of input and output of the ram, referred as Q_1 and Q_2 can be calculated as,

$$Q_1 = Kx_v\sqrt{(P_s - P_1)} \tag{1}$$

$$Q_2 = Kx_v\sqrt{(P_2 - P_o)} \tag{2}$$

where K is a constant determined by the physical characteristics of the valve. The piston motion can be considered as,

$$Q_1 = Q_L + \frac{V_1}{B}\dot{P}_1 + A\dot{Y} \tag{3}$$

$$Q_2 = Kx_v\sqrt{(P_2 - P_o)} \tag{4}$$

where Q_L is the leakage, which is proportional to the pressure difference across the piston. The leakage can be written as,

$$Q_L = K_L(P_1 - P_2) \tag{5}$$

where K_L is constant. The steering torque can be expressed as,

$$T_s = P_L A_e d_j \tag{6}$$

P_L is related to the articulated angle, can be considered as below,

$$P_L = \frac{4A_e d_j}{V_t}\beta_e\theta \tag{7}$$

where V_t is the volume of the hydraulic cylinder, β_e is the elastic modulus. Substituted (7) to (6), the steering torque can be rewritten as,

$$T_s = \frac{4A_e^2 d_j^2}{V_t}\beta_e\theta \tag{8}$$

The steering system can be equivalent to a spring, and the spring stiffness can be written as,

$$K_R = \frac{4A_e^2 d_j^2}{V_t}\beta_e \tag{9}$$

For a general position, the spring stiffness can be written as,

$$K_R = \left(\frac{1}{V_1} + \frac{1}{V_2}\right)A_e^2 d_j^2 \beta_e \tag{10}$$

The torsional damping can be considered at the articulation joint owing to the friction in cylinders and articulation joint. Therefore, the effects of friction and leakage can be equivalent to a torsional damping C_R . The total steering torque in the steering system of the articulated steering vehicle can be written as,

$$M_o = K_R\theta + C_R\dot{\theta} \tag{11}$$

B. Wheel, tire and terrain model

The wheel model in this paper is considered as,

$$I_w\dot{\omega}_w = T_w - F_x R_e - f_r F_z R_e \tag{12}$$

where I_w is the rotational inertia of the wheel; ω_w is the rotation angular acceleration of the tire; T_w is the torque from the drive shift; F_x is the counter longitude force of tire from tire; R_e is the rolling radius of the tire; f_r is the rolling resistance coefficient. The Magic Fila tire model is shown as Figure 3.

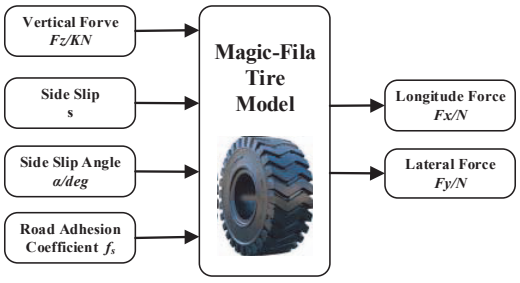

Fig. 4. Structure of MF tire model.

In this model, the tire forces are described as the complex nonlinear function of the tire vertical load, slip rate, and slip angle. Therefore, the 'magic formula' mathematical model, considering the longitudinal force and lateral force, can be written as,

$$\begin{cases} F = D\sin\left[C\arctan\left\{BX - E\left(BX - \arctan\left(BX\right)\right)\right\}\right] + S_v \\ X = x + S_h \end{cases} \tag{13}$$

The long longitudinal force and lateral force can be got as below,

$$\begin{cases} F_x = \dfrac{|\sigma_x|}{\sigma}F_{x0},\ F_y = \dfrac{|\sigma_y|}{\sigma}F_{y0} \\ \sigma_x = -\dfrac{s}{s+1}, \sigma_y = -\dfrac{\tan\alpha}{s+1}, \sigma = \sqrt{\sigma_x^2 + \sigma_y^2} \end{cases} \tag{14}$$

where *B*, *C*, *D*, *E*, *Sv* and *Sh* are the stiffness, shape, peak, curvature, horizontal drift and vertical drift factor, respectively. All of them are described as the function of the tire vertical load, tire slip rate and slip angle.

The vibration caused by the random single of the road is neglected, the terrain model in this paper is consider as,

$$x_{Road} = \{f_r, \alpha\}^T \tag{15}$$

where α is the road slop, f_r is the rolling resistance coefficient.

C. Paremetres estimation module

The parameters estimation module is to estimate the vehicle's driving states, including the following sections.

a) Estimation of tire's slip rate

The longitude tire force is influenced by the side slip in drive mode and break mode, and the side slip can be defined as:

$$s_i = \begin{cases} \dfrac{\omega_w R_w - v_x}{\omega_w R_w}, \omega_w R_w > v_x, \omega_w \neq 0, drive \mod e \\ \dfrac{\omega_w R_w - v_x}{v_x}, \omega_w R_w < v_x, v_x \neq 0, break \mod e \end{cases} \tag{16}$$

b) Estimation of Tire's Side Slip Angle

The estimation equation of side slip angle in SAE tire coordinate system can be described as:

$$\begin{cases} \alpha_f = \arctan\dfrac{v_{yf}}{v_{xf}} \\ \alpha_r = \arctan\dfrac{v_{yr}}{v_{xr}} \end{cases} \tag{17}$$

where α_f and α_r donate the side slip angle of the front and rear tire, respectively.

D. Articulated steering vehicle body model

For the ASV, the vehicle body consists of two rigid sections, each mounted on a single rigid axle and connected by the articulated joint to allow relative movement in yaw. The ASV model incorporates rear axle yaw motion relative to the rear section, by an amount proportional to the articulation angle. This gives the vehicle extra manoeuvrability but also influences the handling behaviour and stability. In this paper, a 4-DOF AVS bicycle model is built based on the d'Alembert's principle. The structure of the bicycle model is shown as Fig. 6. v_{xf} and v_{xr} donate the longitude velocity of front and rear parts; v_{yf} and v_{yr} are the lateral velocities of front and rear sections; ω_f and ω_r are yaw rates of front and rear sections; F_{xf}, F_{yf}, F_{xr}, F_{yr} represent the longitude and lateral tire force of front tire and rear tire respectively; O_f and O_r are the mass center of front rear parts, a and b are the distance from the front axle to front body center of mass , and the distance from the articulated joint to the front body center of mass, respectively; c and d are the distance from the articulated joint to the rear body center of mass, and the distance from the front axle to rear body center of mass, respectively; θ is the articulated angle; M is steering torque generated by steering cylinders, which can be defined as,

$$M = K_R\theta + C_R\dot{\theta} + T_s \tag{18}$$

where K_R is the damp stiffness, C_R is the spring stiffness, T_s is the input steering torque.

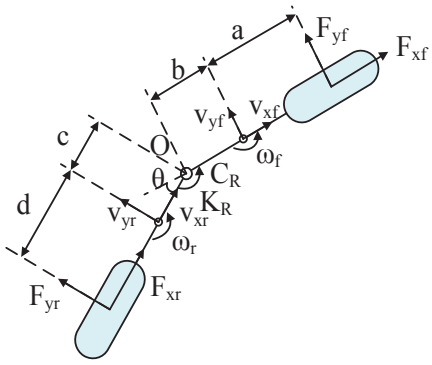

Fig. 5. Stress analysis for ASV.

The active force of the model are the longitude and lateral tire force, the grade resistance and rolling resistance are consider, the wind drag is neglected. The equation of the AS bicycle body model is as below.

$$\begin{cases} F_{yf}(a+b) - bm_f a_{yf} - I_f\dot{\omega}_f + T_s = 0 \\ -F_{yr}(c+d) + cm_r a_{yr} - I_r\dot{\omega}_r - T_s = 0 \\ F_{xf} - m_f a_{xf} + F_{xr}\cos\theta - F_{yr}\sin\theta - m_r a_{xr}\cos\theta + m_r a_{yr}\sin\theta = 0 \\ F_{yf} - m_f a_{yf} + F_{yr}\cos\theta + F_{xr}\sin\theta - m_r a_{yr}\cos\theta - m_r a_{xr}\sin\theta = 0 \end{cases} \tag{19}$$

For a_{xf} and a_{yf} are the longitude and lateral acceleration of front body center of mass, can be described as:

$$\begin{cases} a_{xf} = \dot{v}_{xf} - v_{yf}\omega_f \\ a_{yf} = \dot{v}_{yf} + v_{xf}\omega_f \end{cases} \tag{20}$$

For a_{xr} and a_{yr} are the longitude and lateral acceleration of rear body center of mass, can be described as:

$$\begin{cases} a_{xr} = \dot{v}_{xr} - v_{yr}\omega_r \\ a_{yr} = \dot{v}_{yr} + v_{xr}\omega_r \end{cases} \tag{21}$$

The relationship of ω_r, v_{xr} and v_{yr} can be described as,

$$\begin{cases} \omega_r = \omega_f + \dot{\theta} \\ v_{xr} = v_{xf}\cos\theta + (v_{yf} - b\omega_f)\sin\theta \\ v_{yr} = (v_{yf} - b\omega_f)\cos\theta - v_{xf}\sin\theta - c(\omega_f + \dot{\theta}) \end{cases} \tag{22}$$

The following five state variables are enough to derive the equation motion

$$x = \begin{bmatrix} v_{xf} & v_{yf} & w_f & \theta & \dot{\theta} \end{bmatrix}^T \tag{23}$$

The input of the model is defined as $u = \begin{bmatrix} F_{xf} & F_{xr} & T_s \end{bmatrix}$, the final form of the equation in terms of the state variables can be written as,

$$R(x,u)\dot{x} = F(x,u) \tag{24}$$

where,

$$R(x,u) = \begin{bmatrix} 0 & m_r b & I_f & 0 & 0 \\ m_r c\sin\theta & -m_r c\cos\theta & m_r c^2 + m_r cb\cos\theta + I_r & 0 & m_r c^2 + I_r \\ m_f + m_r & 0 & m_r c\sin\theta & 0 & m_r c\sin\theta \\ 0 & 0 & 0 & 1 & 0 \\ 0 & m_f + m_r & -m_r(b + c\cos\theta) & 0 & -m_r c\cos\theta \end{bmatrix} \tag{25}$$

$$F(x,u) = \begin{bmatrix} F_{yf}(a+b) - m_f b v_{xf}\omega_f + M \\ m_r c\omega_f v_{xf}\cos\theta + m_r c\omega_f v_{yf}\sin\theta - m_r cb\omega_f^2\sin\theta - F_{yr}(c+d) - M \\ F_{xf} + m_f v_{yf}\omega_f + F_{xr}\cos\theta - F_{yr}\sin\theta - cm_r\cos\theta(\omega_f + \dot{\theta})^2 - b\omega_f^2 m_r + \omega_f v_{yf} m_r \\ \dot{\theta} \\ F_{yf} + F_{yr}\cos\theta + F_{xr}\sin\theta - m_f v_{xf}\omega_f - cm_r\sin\theta(\omega_f + \dot{\theta})^2 - \omega_f v_{xf} m_r \end{bmatrix} \tag{26}$$

III. PATH TRACKING FOR ASV

The structure of path tracking for ASV based on weighted PI is shown as Figure 5. The weighted PI control method is applied to path tracking for ASV. The steering torque is determined by the normalized displacement error and heading angle error. The driving torque is determined by the difference of the reference speed and the vehicle driving speed.

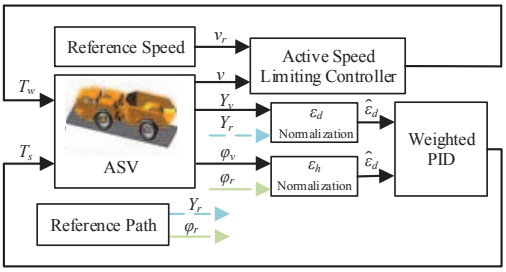

Fig. 6. Structure of path tracking based on weighted PID.

A. Active Speed Limiting Control

The PID controller is applied in the active limiting speed control. And the upper vehicle velocity bound under the anti-sideslip constraints is calculated first. The sideslip constraints describes the maximum vehicle velocity for lateral stability [12, 13]. In simplified analysis, the slip constraints for ASV can be derived as,

$$(m_f + m_r)\bullet a_y \le (m_f + m_r)\bullet\mu\bullet g\bullet\cos\alpha \tag{27}$$

where g is the gravity acceleration, μ and α are the estimated road adhesion coefficient and gradient. In this paper, $\mu = 1$, $\alpha = 0$.

When the vehicle is steering at steady state, it can be approximated that,

$$|a_y| \approx v_x^2 / R \tag{28}$$

where R is the radius of the reference path. Substituted (29) to (28), the upper bound of velocity can be written as,

$$v_{x,upper} \approx \sqrt{\frac{g}{c}} \tag{29}$$

where c is the curvature of the reference path. The top speed of ASV in this paper is $v_{x,\max} = 3.5m/s$ .Therefor, the target of active speed limiting control is to limit the velocity of the vehicle lower than the upper bound and the top speed at the same time, which can be described as,

$$v_{xf} \le \min(v_{x,upper}, v_{x,\max}) \tag{30}$$

B. Weighted PID Stgeering Control

The reference path consist of three primitives: straight, arcs, and clothoid curves. If the curvature of the each path is known, the tangent direction along the path, or heading, and the positions along the path can be expressed as [14],

$$\varphi = \int_0^s k(z)dz + \varphi_0 \tag{31}$$

$$x(s) = \int_0^s \cos(\varphi(z))dz + x_0 \tag{32}$$

$$y(s) = \int_0^s \sin(\varphi(z))dz + y_0 \tag{33}$$

where s is defined as the driving distance. Therefore, the heading angle and coordinate information of reference path can be found by lookup table by driving distance.

As shown in Fig.6, the path tracking error consist of displacement error and heading angle error. The displacement error is defined as the distance between the reference point and the center of the front axle of ASV in Y direction. The heading angle error is defined as the difference of vehicle heading angle and the tangent of the reference point. The desire steering torque can be considered as,

$$T_{s,des} = wT_{s,yerr} + (1-w)T_{s,herr} \tag{34}$$

where $T_{s,des}$ referred to the desire steering torque, $T_{s,\mathrm{yerr}}$ and $T_{s,herr}$ referred to the steering torque created by the displacement error and heading angle error respectively. The weighted parameter is referred as w .

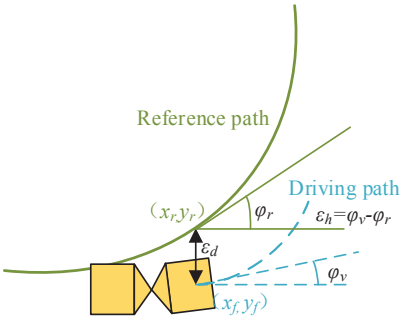

Fig. 7. Path tracking error.

In this paper, the tolerance of displacement error and heading angle error are set to [-0.5, 0.5] (m), and [-0.15, 0.15] (rad) respectively. Therefore, the displacement error and heading angle error can be normalized as,

$$\hat{\varepsilon}_d = \frac{\varepsilon_d - (-0.5)}{0.5 - (-0.5)} \tag{35}$$

$$\hat{\varepsilon}_h = \frac{\varepsilon_h - (-0.15)}{0.15 - (-0.15)} \tag{36}$$

The weighted parameter can be expressed as,

$$w = \frac{\hat{\varepsilon}_d}{\hat{\varepsilon}_d + \hat{\varepsilon}_h} \tag{37}$$

Substituted (34) to (31), the desire steering torque can be rearranged as,

$$T_{s,des} = \frac{\hat{\varepsilon}_d}{\hat{\varepsilon}_d + \hat{\varepsilon}_h} T_{s,yerr} + \frac{\hat{\varepsilon}_h}{\hat{\varepsilon}_d + \hat{\varepsilon}_h} T_{s,herr} \tag{38}$$

IV. Simulation Result and Analysis

The simulation platform is set up based on a 35 tone mining truck, and the parameters of the ASV for simulation is shown in table 1.

TABLE I. PARAMETERS OF THE ASV

Name	Symbol	Value	Unite
Mass of vehicle body	m_f m_r	21772, 12688	Kg
Moment of inertia of vehicle body	I_f I_r	30000, 35000	Kgm^2
C.G Position parameters	a b c d	-0.394, 2.074, 2.033, 1.406	m
Wheel Rolling Radius	R_w	1	m
Moment of inertia of wheel	I_w	750	Kgm^2
Spring stiffness	K_R	300000	Nm/rad
Torsional stiffness	C_R	50000	Nms/rad

For simulation, a lane change path was planned. Fig. 8 shows the curvature of the reference path, which is continuous, with maximum and minimum curvature as 0.06 and -0.06. Fig. 9 shows the path tracking result, in which the blue line and red line refer to the reference path and driving path respectively. Fig. 10 shows the relationship of vehicle speed and driving distance. Fig. 11 and Fig. 12 show the heading angle error and displacement error respectively. Fig. 13 shows the weighted coefficient during the vehicle's driving. The result shows the ASV can track the reference path and velocity very well based active speed limiting control and weighted PID

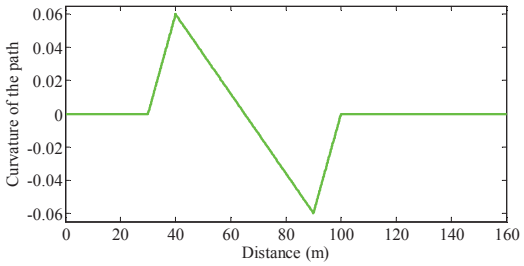

Fig. 8. Curvature of the reference path.

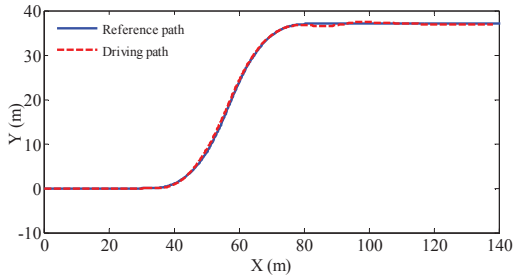

Fig. 9. Path tracking result.

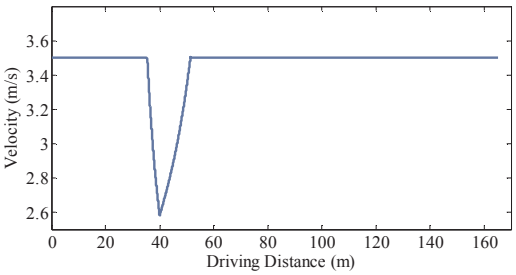

Fig. 10. Vehicle velocity of ASV.

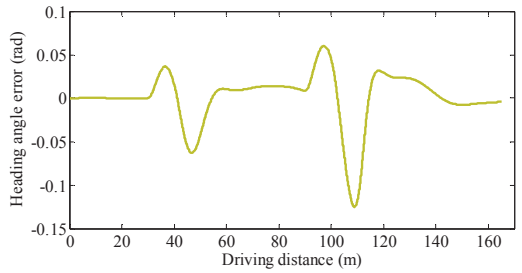

Fig. 11. Heading angle error of path tracking.

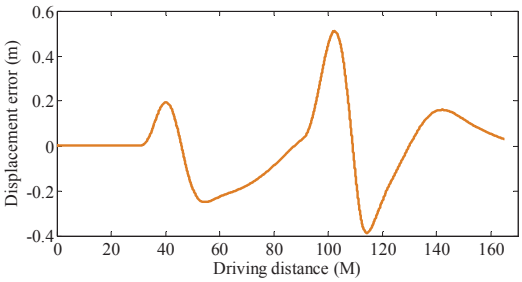

Fig. 12. Displacement error of path tracking.

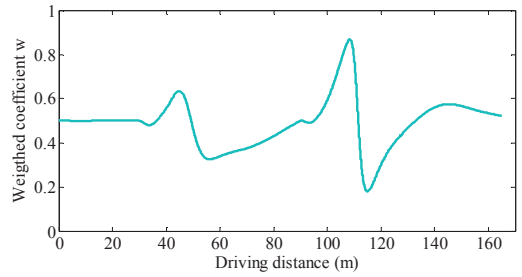

Fig. 13. Weighted coefficient of PID controller.

V. Conclusion

In this paper, the integrated ASV dynamics model was built in Matlab/Simulink. The active speed limiting control and weighted PID path tracking module are designed based on the AV's path tracking error. The efficiency and sensitivity of the proposed path tracking control scheme have been validated through the Matlab simulation. The future work should be focused on the experimental verification of the real performance of the proposed path-tracking controller.

References

[1] N. Vagenas, M. Scoble and G. Baiden, "A review of the first 25 years of machine automation in underground hard rock mines," CIM Bulletin, vol. 90, pp. 57-62, 1997.

[2] Hannu Makela, "Overview of LHD navigation without artificial beacons," Robtics and Autonomous System, vol. 36, pp. 21-35, 2001.

[3] Roberts, Jonathan M., P. Corke, Cunningham J. and Durrant-Whyte H., "Automation of underground LHD and truck haulage," AusIMM Annual Conference, Australia, pp. 241-246, 1998.

[4] Peter Ridley and Peter Corke, "Load haul dump vehicle kinematics and control," Transactions on ASME, vol. 125, pp. 54-59, 2003.

[5] B.J. Dragt, "An overview of the automation of LHD vehicles in an underground mining environment," 16th Triennial World Congress, Prague, vol. 38, pp. 37-48, 2005.

[6] Y. Yavin, "Modelling the motion of an underground mining vehicle," Mathematical and Computer Modelling, vol. 42, pp. 1123-1130, 2005.

[7] Thaker Nayl, George Nikolakopoulos and Thomas Gustafsson, "Effect of kinematic parameters on MPC based on-line motion planning for an articulated vehicle," Robotics and Autonomous Systems, vol.70, pp.16-24, 2015.

[8] F. Rovira-Más, and Q. Zhang, "Fuzzy logic control of an electrohydraulic valve for auto-steering off-road vehicles," Journal of Automobile Engineering, vol. 222, pp. 917-934, Jun, 2008.

[9] Nasser Lashgarian Azad , Amir Khajepour and John Mcphee, "Robust state feedback stabilization of articulated steer vehicles," Vehicle System Dynamics, vol. 45, pp. 249–275, 2008.

[10] S. H. Tabatabaei Oreh, R. Kazemi, and S. Azadi, "A sliding-mode controller for directional control of articulated heavy vehicles," Journal of Automobile Engineering , vol. 228, pp. 245-262, 2014.

[11] F. Rovira-Más, and Q. Zhang, "Fuzzy logic control of an electrohydraulic valve for auto-steering off-road vehicles," Journal of Automobile Engineering, vol. 222, pp. 917-934, 2008.

[12] K. Nam, S. Oh, H. Fujimoto, and Y. Hori, "Robust yaw stability control for electric vehicles based on active front steering control through a steer-by-wire system," International Journal of Automotive Technology, vol. 13, pp. 1169-1176, 2012.

[13] Wei Liu, Hongwen He, Fengchun Sun and Jiangyi Lv, "Integrated chassis control for a three-axle electric bus with distributed driving motors and active rear steering system," Vehicle System Dynamics, vol. 55, pp 601-625, 2017.

[14] Rajamani R, Piyabongkarn D, Lew JY, et al. "Tire-road friction-coefficient estimation," IEEE Control System, vol. 30, pp. 54–69, 2010.

[15] Joseph Funke and J. Christian Gerdes, "Simple clothoid lane change trajectories for automated vehicles incorporating friction constraints," Journal of Dynamic Systems, Measurement, and Control, vol, 138, 2015.